VOLUME 35 · NUMBER 19 · JULY 1, 2017

JOURNAL OF CLINICAL ONCOLOGY

ORIGINAL REPORT

# Ultrasound Molecular Imaging With BR55 in Patients With Breast and Ovarian Lesions: First-in-Human Results

*Jürgen K. Willmann, Lorenzo Bonomo, Antonia Carla Testa, Pierluigi Rinaldi, Guido Rindi, Keerthi S. Valluru, Gianluigi Petrone, Maurizio Martini, Amelie M. Lutz, and Sanjiv S. Gambhir*

Author affiliations and support information (if applicable) appear at the end of this article.

Published at jco.org on March 14, 2017.

Clinical trial information: 2012-000699-40.

Corresponding author: Jürgen K. Willmann, MD, Department of Radiology, Molecular Imaging Program at Stanford, Stanford University, 300 Pasteur Dr, Room H1307, Stanford, CA 94305-5621; e-mail: willmann@stanford.edu.



0732-183X/17/3519w-2133w/$20.00

## ABSTRACT

### Purpose

We performed a first-in-human clinical trial on ultrasound molecular imaging (USMI) in patients with breast and ovarian lesions using a clinical-grade contrast agent (kinase insert domain receptor [KDR] –targeted contrast microbubble [$MB_{KDR}$]) that is targeted at the KDR, one of the key regulators of neoangiogenesis in cancer. The aim of this study was to assess whether USMI using $MB_{KDR}$ is safe and allows assessment of KDR expression using immunohistochemistry (IHC) as the gold standard.

### Methods

Twenty-four women (age 48 to 79 years) with focal ovarian lesions and 21 women (age 34 to 66 years) with focal breast lesions were injected intravenously with $MB_{KDR}$ (0.03 to 0.08 mL/kg of body weight), and USMI of the lesions was performed starting 5 minutes after injection up to 29 minutes. Blood pressure, ECG, oxygen levels, heart rate, CBC, and metabolic panel were obtained before and after $MB_{KDR}$ administration. Persistent focal $MB_{KDR}$ binding on USMI was assessed. Patients underwent surgical resection of the target lesions, and tissues were stained for CD31 and KDR by IHC.

### Results

USMI with $MB_{KDR}$ was well tolerated by all patients without safety concerns. Among the 40 patients included in the analysis, KDR expression on IHC matched well with imaging signal on USMI in 93% of breast and 85% of ovarian malignant lesions. Strong KDR-targeted USMI signal was present in 77% of malignant ovarian lesions, with no targeted signal seen in 78% of benign ovarian lesions. Similarly, strong targeted signal was seen in 93% of malignant breast lesions with no targeted signal present in 67% of benign breast lesions.

### Conclusion

USMI with $MB_{KDR}$ is clinically feasible and safe, and KDR-targeted USMI signal matches well with KDR expression on IHC. This study lays the foundation for a new field of clinical USMI in cancer.

*J Clin Oncol 35:2133-2140. © 2017 by American Society of Clinical Oncology*

## INTRODUCTION

Ultrasound is a widely available, portable, and relatively inexpensive imaging modality used as a first-line imaging technique in patients with suspected breast or ovarian lesions.[1,2] The introduction of molecularly targeted contrast microbubbles that can bind to certain molecules expressed in cancer has made ultrasound a molecular imaging modality that allows improved detection, characterization, and monitoring of cancer in preclinical studies.[3-8]

Contrast microbubbles are micron-sized, purely intravascular contrast agents consisting of a gaseous core contained by a shell. By functionalizing the shell with binding ligands to certain molecules, microbubble-enhanced ultrasound can visualize molecules such as kinase insert domain receptor (KDR), one of the key regulators of neoangiogenesis differentially expressed in various cancers including breast and ovarian cancer.[9-14] Several preclinical studies have shown that KDR-targeted ultrasound molecular imaging (USMI) is a promising technique for cancer imaging.[15-20] In those early preclinical studies, with one exception,[21] biotinylated ligands (used to bind to KDR or other targets) were attached to streptavidin-containing microbubble shells through biotin-streptavidin interactions. However,

ASSOCIATED CONTENT

See accompanying Editorial on page 2101

Data Supplement
DOI: https://doi.org/10.1200/JCO.2016.70.8594

DOI: https://doi.org/10.1200/JCO.2016.70.8594

because streptavidin is immunogenic and can cause severe allergic reactions in patients,[22,23] USMI using these first-generation targeted contrast agents in patients has not thus far been translated to clinical practice. Recently, a novel clinical-grade KDR-targeted contrast microbubble ($MB_{KDR}$) has been designed by incorporating KDR-binding phospholipid-heteropeptides into lipid-shelled microbubbles without the use of biotin or streptavidin, and strong accumulation of $MB_{KDR}$ has been shown in various preclinical cancer models.[24-31] The purpose of this study was to clinically translate USMI using $MB_{KDR}$ in a first-in-human clinical trial in patients with breast and ovarian lesions (Fig 1).

## METHODS

### Study Design and Sample

This exploratory-phase, single-center, open-label, prospective, Health Insurance Portability and Accountability Act–compliant clinical study was approved by the local institutional review board, and informed consent was obtained from all patients. Between October 2012 and April 2014, patients referred to undergo surgery or biopsy of an ovarian or breast lesion were invited to participate in this clinical study (for more details on patient inclusion and methods, see Data Supplement). Twenty-four postmenopausal (ie, no menstrual period for at least 1 year) or perimenopausal women with ovarian lesions and 21 women with breast lesions scheduled for surgery or biopsy within 30 days after enrollment were included. Inclusion and exclusion criteria are summarized in the Data Supplement.

### Procedures

$MB_{KDR}$ (BR55; Bracco, Geneva, Switzerland) was good manufacturing practice (GMP) synthesized as described previously.[24,25] Patients were monitored for any untoward medical occurrences from the time of signing the informed consent through 72 hours after intravenous contrast agent administration. All patients underwent baseline vital signs, pulse oximetry, ECG, blood tests, urinalysis, and, if applicable, β-human chorionic gonadotropin testing.

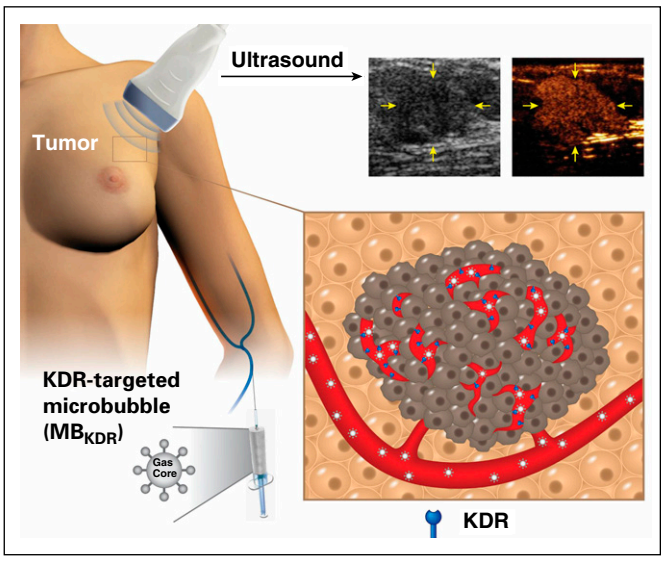


**Fig 1.** Schematic shows basic concept of ultrasound molecular imaging (USMI) in patients with breast cancer. Kinase insert domain receptor (KDR) –targeted contrast microbubbles ($MB_{KDR}$) containing a gas core are injected intravenously. While $MB_{KDR}$ bubbles freely circulate in the vasculature, they attach to the breast cancer neovasculature overexpressing KDR (shown as blue receptor). Using clinical ultrasound equipment, the accumulation of $MB_{KDR}$ in breast cancer (yellow arrows) can be seen as strong signal on contrast mode image (right). Note that the brightness mode is shown to the left of the contrast mode image for anatomic reference.

For breast imaging, an Acuson Sequoia 512 (Siemens, Munich, Germany) clinical ultrasound scanner with a 15L8 transducer and, for ovarian imaging, a MyLab clinical ultrasound machine (Esaote, Florence, Italy) with an endocavitary 1123 transducer were used. Target lesions were first identified in bright (B) mode imaging followed by Doppler imaging. Imaging was then switched to contrast mode, and the transducer was kept at a location of the largest solid component in ovarian lesions and through the maximum central diameter of breast lesions. $MB_{KDR}$ was then manually bolus injected over a 10-second period, and USMI images were obtained continuously for 45 seconds to document $MB_{KDR}$ arrival in the target lesion. Ten-second imaging clips were then obtained at 5 minutes after $MB_{KDR}$ injection and then every 2 minutes until 29 minutes. $MB_{KDR}$ was injected in three distinct patient groups each at three different doses (0.03 mL/kg of body weight [bw], 0.05 mL/kg bw and 0.08 mL/kg bw), according to a predefined dose-escalation design. Each patient received one injection of the contrast agent at the assigned dose (Data Supplement).

Qualitative USMI analysis was performed by two radiologists in consensus, who were blinded to all clinical information except that patients were suspected to have either a breast or ovarian lesion. Both radiologists visually assessed stationary contrast enhancement likely representing binding of $MB_{KDR}$ to its target KDR (defined as focal enhancement still visible after freely circulating microbubbles had disappeared) on images acquired at all time points. Presence of focal enhancement was graded using the following three-grade visual scale: strong (well-defined and strong visual stationary targeted imaging signal), weak (enhancement is weak but considered stationary), or no enhancement (no focal stationary targeted imaging signal was detected in comparison with the rest of the organ). For breast lesions, because presumed normal surrounding breast tissue was available as control tissue within the field of view, quantitative analysis of the signal-to-background ratio (SBR) between the breast target lesion and surrounding breast tissue was also calculated. This quantitative analysis was not performed for the ovary data sets because normal ovarian tissue could not be definitively identified within the field of view for most of the target ovarian lesions.

After biopsy or surgery, standard protocols for collecting formalin-fixed, paraffin-embedded tissue were followed, and the tissues were stained with hematoxylin and eosin[32] for histologic diagnosis. For immunohistochemical (IHC) analysis, consecutive tissue sections were stained for the vascular endothelial cell marker CD31 and for KDR. Semiquantitative IHC analysis of KDR expression was performed by two pathologists in consensus, and the grading system comprised the assessment of both intensity of the IHC signal per vessel and the estimate of the number of stained vessels per microscopic field at ×400. KDR staining was graded using the following four-point visual assessment score: no staining (no vessel stained); weak staining (few vessels stained with faint signal); moderate staining (most vessels stained with weak or moderate signal); and high staining (all vessels stained with strong signal).

At the conclusion of the independent blinded analysis of both USMI and pathology findings, one pathologist and the two radiologists matched the semiquantitative results of the two independent blinded readings in a consensus reading session. Specifically, the results were deemed to be matched if the following conditions were met: when USMI signal was strong or weak and KDR staining was high or moderate or when USMI signal was none and KDR staining was weak or none. See the Data Supplement for more information on methods used in this study.

### Statistical Analysis

The sample size was defined to comply with the recent International Council for Harmonisation[33] recommendations for exploratory clinical trials to explore KDR-targeted USMI to visualize KDR expression in ovarian and breast lesions. Fisher's exact *t* tests were performed on the data

  

to determine whether increasing dosage results in increased binding. Differences in binding duration among dosage levels were tested using an exact Kruskal-Wallis test stratified by tissue type (breast or ovary). $P \leq .05$ was considered statistically significant, and tests were performed using SAS Version 9.1.3 (SAS Institute, Cary, NC).

## RESULTS

Demographic and clinical characteristics of the 45 patients imaged with $MB_{KDR}$ are provided in the Data Supplement.

### Clinical Safety

Twelve (27%) of 45 patients reported 15 adverse events that were mild or moderate in intensity (Data Supplement); of these 12 patients, five (42%) had ovarian lesions and seven (58%) had breast lesions. No serious adverse events were reported, no patient died during the study, and no patient discontinued study participation as a result of an adverse event. In patients with ovarian lesions, none of the reported adverse events was considered by the local investigator to be related to $MB_{KDR}$ administration. In three patients with breast lesions, four adverse events were considered to be related to $MB_{KDR}$ administration. One patient reported lip pruritus and oral discomfort; both events were mild in intensity. One patient reported subjective hypertension of mild intensity, and one patient reported headache of moderate intensity. All patients recovered without sequelae and without any intervention.

No abnormal changes in physical examination results were observed from before to 24 hours after $MB_{KDR}$ administration. Similarly, no clinically significant changes from baseline in vital signs and ECG results were recorded after the administration of $MB_{KDR}$ (Data Supplement). Regarding laboratory values, the following three patients had a change from baseline value that was outside the predefined change limits: one patient showed an increase in RBC count from 5.5 to 6.3 $\times 10^{12}$/L; in one patient, AST increased from 33 to 44 U/L; and one patient with a baseline glucose value outside of normal limits showed an increase in blood glucose from 5.9 to 11.7 mmol/L. All changes were reported at 24 hours after $MB_{KDR}$ administration. None of the changes was considered to be clinically significant by the local investigator.

### Feasibility of KDR-Targeted USMI and Comparison With Immunofluorescence

Clinical USMI using $MB_{KDR}$ was feasible in all patients on the clinically available equipment used in this study. In all patients, successful intravenous administration of the $MB_{KDR}$ with enhancement of the solid portion of the ovarian and breast target lesions during the bolus phase within the first 45 seconds was observed.

*Ovarian lesions.* Table 1 lists the histologic diagnoses of ovarian target lesions. Twenty-two (92%) of 24 target lesions were confirmed in the ovaries during surgery and used for further analysis. Two (8%) of 24 lesions were intraoperatively found outside the ovaries (a benign pedunculated necrotic/hemorrhagic uterine nodule and a benign hematosalpinx) and, therefore, were excluded from the data analysis. Benign lesions were found in nine (41%) of 22 target ovaries (four in left ovaries and five in right ovaries) with a mean size of 1.86 cm (range, 0.7 to 3.7 cm). Malignant lesions were present in 13 (59%) of 22 target ovaries (four in left ovaries and nine in right ovaries) with a mean size of 5.38 cm (range, 1.2 to 10.0 cm); one of the malignant lesions in the right ovary was not a primary ovarian lesion but a metastasis from a neuroendocrine GI tumor. Overall, KDR-targeted USMI and KDR IHC signals matched in 19 (86%) of 22 ovarian lesions (95% CI, 65% to 97%), including eight (89%) of the nine benign lesions

**Table 1.** Summary of Matching Results in Ovarian Target Lesions for Various Histologies

| Target Ovary Histology | No. of Lesions | | |
|---|---|---|---|
| | Match: Yes | Match: No | Total |
| Malignant | 11 | 2 | 13 |
| Clear cell carcinoma | | | |
| Signal: Strong | | | |
| Staining: Moderate | 1 | | 1 |
| Endometrioid carcinoma | | | |
| Signal: Strong | | | |
| Staining: High | 1 | | 1 |
| Staining: Moderate | 2 | | 2 |
| Solid high-grade cystadenocarcinoma | | | |
| Signal: Strong | | | |
| Staining: High | 1 | | 1 |
| Granulosa cell carcinoma | | | |
| Signal: Strong | | | |
| Staining: Moderate | 1 | | 1 |
| Metastasized neuroendocrine (GI) tumor | | | |
| Signal: None | | | |
| Staining: Weak | 1 | | 1 |
| High-grade serous cystadenocarcinoma | | | |
| Signal: Strong | | | |
| Staining: High | 1 | | 1 |
| Staining: Moderate | 2 | | 2 |
| Low-grade serous cystadenocarcinoma | | | |
| Signal: Strong | | | |
| Staining: Weak | | 1 | 1 |
| Borderline serous tumor | | | |
| Signal: None | | | |
| Staining: Weak | 1 | | 1 |
| Mucinous cystadenocarcinoma | | | |
| Signal: None | | | |
| Staining: Moderate | | 1 | 1 |
| Benign | 8 | 1 | 9 |
| Mature cystic teratoma | | | |
| Signal: Strong | | | |
| Staining: Moderate | 1 | | 1 |
| Signal: None | | | |
| Staining: Weak | 1 | | 1 |
| Leiomyoma | | | |
| Signal: None | | | |
| Staining: Weak | 1 | | 1 |
| Brenner tumor | | | |
| Signal: None | | | |
| Staining: Weak | 1 | | 1 |
| Mucinous cystadenofibroma | | | |
| Signal: Strong | | | |
| Staining: Moderate | 1 | | 1 |
| Serous cystadenofibroma | | | |
| Signal: None | | | |
| Staining: Weak | 3 | | 3 |
| Sclerosing corpus luteum | | | |
| Signal: None | | | |
| Staining: Moderate | | 1 | 1 |
| All malignant and benign lesions combined | 19 | 3 | 22 |

(95% CI, 52% to 99%) and 11 (85%) of 13 malignant lesions (95% CI, 55% to 98%). The one benign lesion without matching (sclerosing corpus luteum) showed moderate KDR staining but no KDR-targeted USMI signal. Similarly, the two malignant lesions without matching (a mucinous cystadenocarcinoma and a borderline serous tumor) showed moderate KDR staining but no KDR-targeted USMI signal. Strong KDR-targeted USMI signal was present in most primary ovarian cancer lesions (10 of 13 lesions; 77%; Figs 2A to 2E; Data Supplement). No targeted signal was seen in most benign lesions (seven of nine lesions; 78%; Figs 2F to 2J; Data Supplement); in one benign teratoma and one benign mucinous cystadenofibroma, KDR-targeted USMI signal was observed.

*Breast lesions.* Table 2 lists the histologic diagnoses of 18 (86%) of 21 breast target lesions and the findings of the corresponding surrounding control breast tissue superior and inferior to the target lesions. Three (14%) of 21 lesions were excluded from data analysis as a result of data storage issues (n = 1) or technical problems (n = 2) during the early technical optimization phase. Histology showed benign lesions in three (17%) of 18 and malignant lesions in 15 (83%) of 18 target breast tissues. In 26 (72%) of 36 breast tissues obtained superficially (n = 12) or deeply (n = 14) to the target lesions, histology showed normal breast tissue. In the remaining 10 (28%) of 36 tissues, the tissue samples collected were too close to the target lesions (< 2 cm) and hence were not analyzed. Overall, KDR-targeted USMI and KDR IHC signals matched in 16 (89%) of 18 breast lesions (95% CI, 89% to 99%), including in two (67%) of three benign lesions (95% CI, 9% to 99%) and 14 (93%) of 15 malignant lesions (95% CI, 68% to 99%). The one benign lesion without matching (a fibroadenoma) showed moderate KDR staining and no KDR-targeted USMI signal. Similarly, the one malignant lesion (ductal adenocarcinoma) without matching showed moderate KDR staining and no KDR-targeted USMI signal. Stationary KDR-targeted USMI signal was present in 14 (93%) of 15 malignant breast lesions (Figs 3A to 3E and 4A to 4I; Data Supplement). In one of the three benign lesions (fibrous mastopathy), there was strong targeted signal, whereas in the other two benign lesions (fibroadenomas), no KDR-targeted signal was seen (Figs 3F to 3J). The mean size of the malignant lesions was 1.64 cm (range, 0.9 to 2.4 cm), whereas the mean size of the benign lesions was 1.83 cm (range, 1.5 to 2.0 cm). KDR staining matched in 26 (100%) of 26 tissues with no KDR-targeted USMI signal seen in the normal control breast tissue surrounding the target lesions. Mean SBR in malignant breast lesions was 1.96 (range, 1.25 to 5.27), whereas in the one benign lesion with strong KDR-targeted USMI signal (fibrous mastopathy), the SBR was 1.2. In 11 (79%) of 14 malignant lesions with strong signal enhancement, the mean SBR was 2.13 (range, 1.25 to 5.27), whereas in three (21%) of 14 malignant lesions with weak signal enhancement, the mean SBR was 1.34 (range, 1.25 to 1.4). In

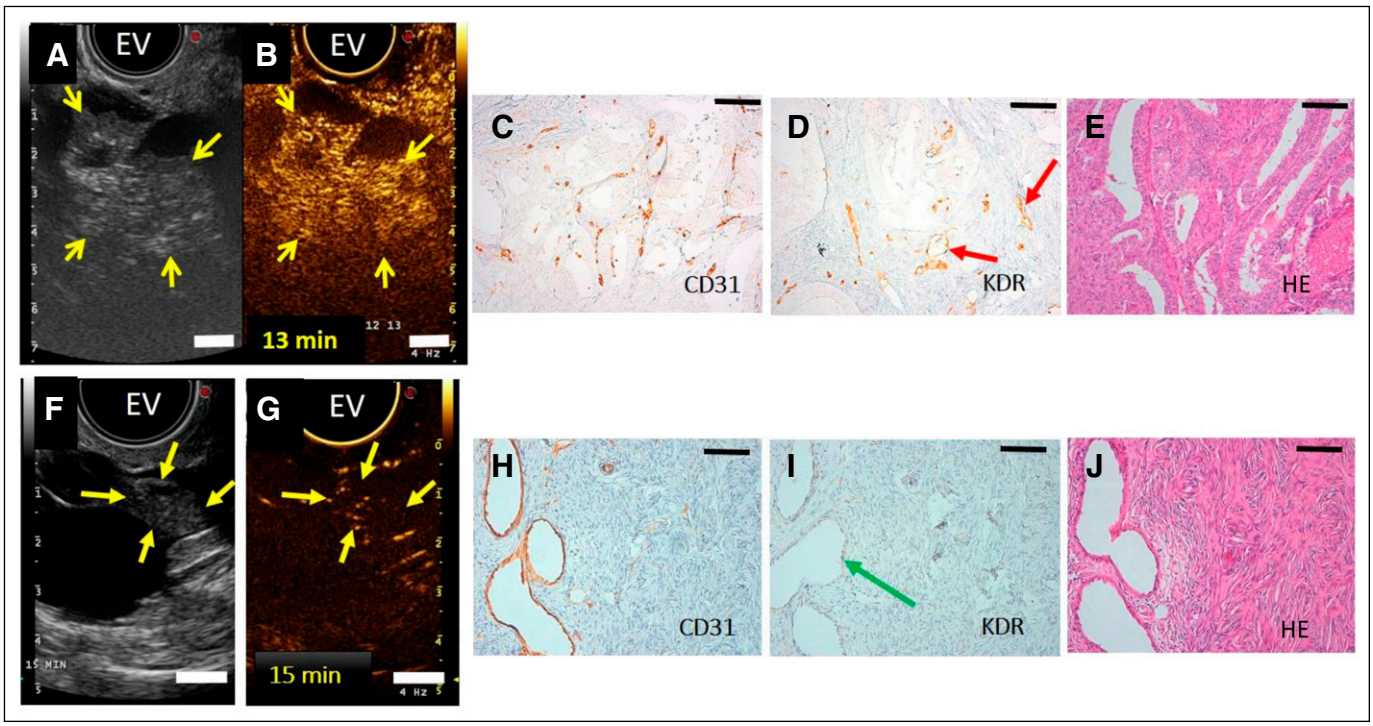


**Fig 2.** Kinase insert domain receptor (KDR) –targeted ultrasound molecular imaging of ovarian lesions. (A) Transverse endovaginal (EV) low mechanical index reference B-mode ultrasound image of the right ovary in a 50-year-old woman shows a 5.2-cm cystic and solid lesion (yellow arrows point to solid portion). (B) Thirteen minutes after intravenous administration of KDR-targeted contrast microbubbles ($MB_{KDR}$), strong imaging signal is seen in the solid portion of the lesion (yellow arrows) on contrast mode ultrasound molecular image. (C and D) Immunohistochemistry performed on consecutive tissue sections demonstrates strong KDR expression on tumor-associated (CD31-positive) neovasculature (red arrows). (E) Histology shows endometrioid carcinoma. (F) Transverse endovaginal low mechanical index reference B-mode ultrasound image of right ovary shows 4.8-cm cystic and solid ovarian lesion (yellow arrows point to solid portion) in a 65-year-old woman. (G) Fifteen minutes after intravenous administration of $MB_{KDR}$, only minimal background signal is seen in 1.3-cm solid part of the lesion (yellow arrows) on contrast mode ultrasound molecular imaging. (H and I) Immunohistochemistry demonstrates minimal KDR expression (green arrow) on CD31-positive vasculature. (J) Histology shows benign serous cystadenofibroma. Scale bar is 1 cm on the ultrasound images and 100 μm on hematoxylin and eosin (HE), CD31, and KDR immunohistochemistry images assessed at ×400 magnification.

  

**Table 2.** Summary of Matching Results in Breast Lesions for Various Histologies

| Breast Histology | No. of Lesions | | |
|---|---|---|---|
| | Match: Yes | Match: No | Total |
| Malignant | 14 | 1 | 15 |
| Ductal adenocarcinoma | | | |
| Signal: Strong | | | |
| Staining: High | 7 | | 7 |
| Staining: Moderate | 4 | | 4 |
| Signal: Weak | | | |
| Staining: Moderate | 3 | | 3 |
| Signal: None | | | |
| Staining: Moderate | | 1 | 1 |
| Benign | 2 | 1 | 3 |
| Fibroadenoma | | | |
| Signal: None | | | |
| Staining: Moderate | | 1 | 1 |
| Staining: Weak | 1 | | 1 |
| Fibrous mastopathy | | | |
| Signal: Strong | | | |
| Staining: Moderate | 1 | | 1 |
| All malignant and benign lesions combined | 16 | 2 | 18 |

addition, when only the maximum SBR values for each patient were considered (the highest SBR value obtained at any time point after intravenous injection of $MB_{KDR}$ for each patient), the mean SBR of all 14 malignant lesions was 2.63 (range, 1.47 to 7.96).

### *Duration of USMI Signal*

At 13 minutes after $MB_{KDR}$ injection, 23 (96%) of 24 ovarian and breast cancers could be seen on USMI (10 of 10 ovarian cancers and 13 of 14 breast cancers; Fig 4; Data Supplement), and USMI signal was detectable up to 29 minutes (the longest tested time point; Fig 4). Increasing dosage did not show a significant difference ($P = .91$) on binding ability of microbubbles in both patient groups with breast and ovarian lesions. In addition, when the effect of dosage was evaluated against the binding duration, the duration of the KDR-targeted USMI signal was not significantly different ($P = .91$) among the three contrast dosing groups.

## DISCUSSION

This study shows, for the first time to our knowledge, that USMI of KDR expression using $MB_{KDR}$ is safe and feasible in women with

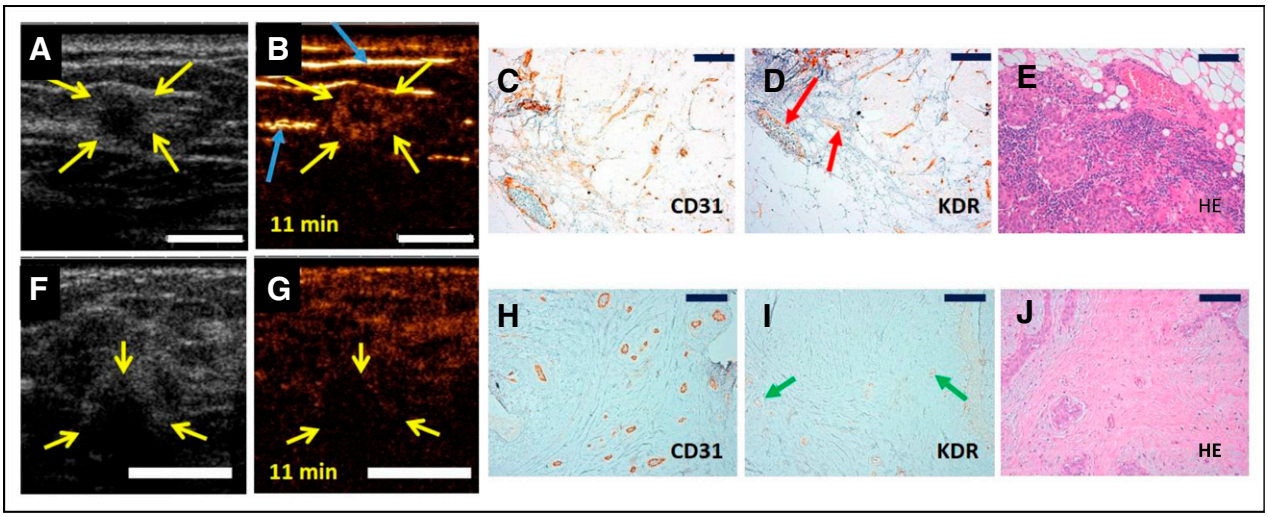


**Fig 3.** Kinase insert domain receptor (KDR) –targeted ultrasound molecular imaging of breast lesions. (A) Transverse B-mode ultrasound image of a 0.9-cm hypoechoic solid lesion (yellow arrows) in the upper inner quadrant of the right breast in a 57-year-old woman. (B) Eleven minutes after intravenous administration of KDR-targeted contrast microbubbles ($MB_{KDR}$), strong stationary imaging signal (yellow arrows) is seen on contrast mode ultrasound molecular image. Note that the linear bright lines seen at tissue interfaces represent tissue leakage artifacts (blue arrows). (C and D) Immunohistochemistry shows strong KDR expression (red arrows) on CD31-positive tumor-associated neovasculature. (E) Histology demonstrates ductal adenocarcinoma. (F) Transverse low mechanical index reference B-mode image in a 36-year-old woman with 2.1-cm hypoechoic solid lesion (yellow arrows) in the upper outer quadrant of the right breast. (G) No stationary signal (yellow arrows) is demonstrated on contrast mode ultrasound molecular image obtained 11 minutes after intravenous injection of $MB_{KDR}$. (H and I) Immunohistochemistry shows faint KDR expression on CD31-positive vasculature (green arrows). (J) Histologic diagnosis was benign fibroadenoma. Scale bar is 1 cm on ultrasound images and 100 μm on hematoxylin and eosin (HE), CD31, and KDR immunohistochemistry images assessed at ×400 magnification.

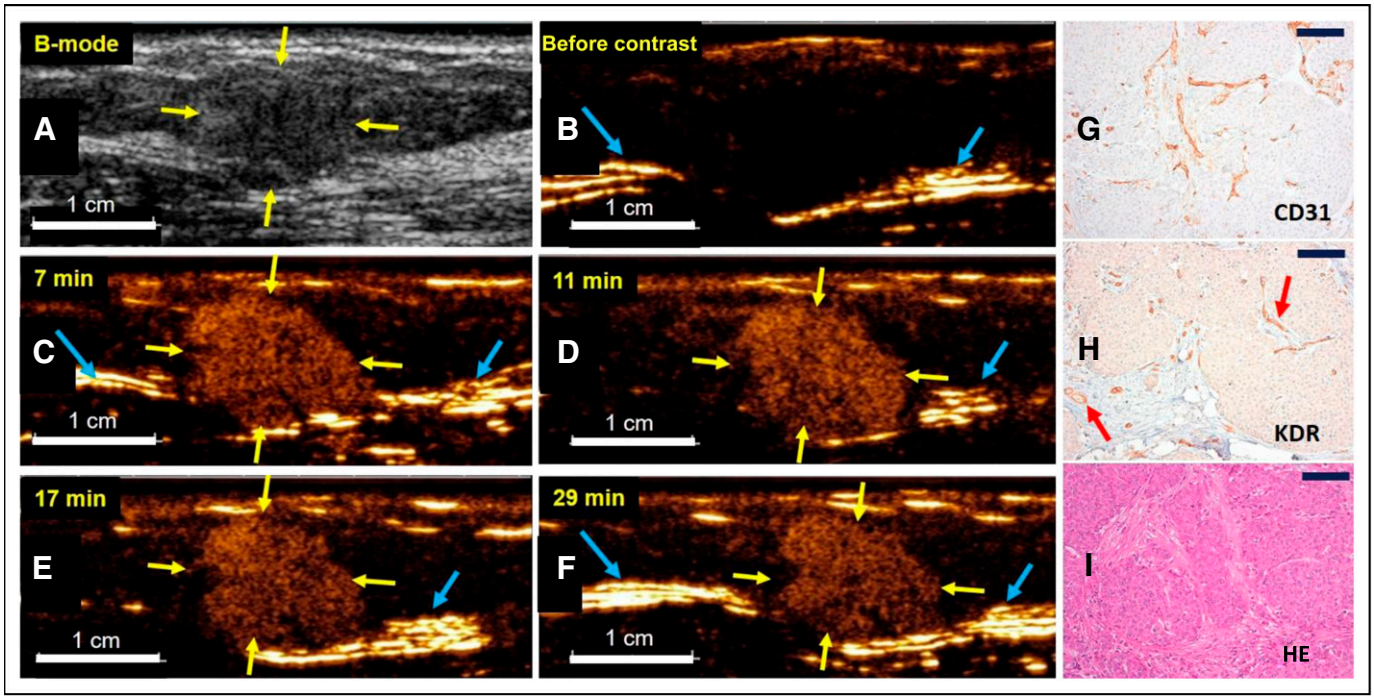


**Fig 4.** Duration of kinase insert domain receptor (KDR) –targeted ultrasound molecular imaging in a 59-year-old woman with ductal adenocarcinoma (yellow arrows) located in the upper external quadrant of the right breast. (A) Transverse B-mode image shows a 1.45-cm heterogeneous isoechoic solid lesion (yellow arrows) within the mammary gland. (B) On a contrast mode image obtained before contrast agent administration, there is no signal in the lesion or surrounding normal breast tissue. Note tissue leakage artifacts (caused by nonlinearities in the front-end electronics of ultrasound machines; blue arrows) as a result of high echo amplitudes at tissue interfaces. (C-F) Transverse contrast mode images obtained at four representative time points up to 29 minutes after intravenous administration of KDR-targeted contrast microbubbles ($MB_{KDR}$) show strong and persistent targeted ultrasound image signal in breast cancer and low background signal. (G and H) Corresponding immunohistochemistry performed on consecutive tissue sections shows multiple CD31-stained tumor vessels and strong neovascular KDR expression in tumor vessels inside the tumor stroma (red arrows). (I) Histology shows ductal adenocarcinoma. Scale bar is 1 cm on ultrasound images and 100 μm on hematoxylin and eosin (HE), CD31, and KDR immunohistochemistry images assessed at ×400 magnification.

ovarian and breast lesions. KDR-targeted USMI signal matches well with KDR expression at IHC, and targeted signal could be seen up to 29 minutes after intravenous injection, the maximum time tested in this study. This study lays the foundation for further clinical development of USMI in oncologic imaging.

Overall, the safety profile of $MB_{KDR}$ was good, with mild or moderate self-resolving subjective adverse events considered related to the $MB_{KDR}$ administration in only three (6.7%) of 45 patients, which is within a comparable range of reported adverse event rates in controlled clinical trials using US Food and Drug Administration–approved, non–molecularly targeted contrast agents (16.8% for perflutren protein-type A microbubbles,[34] 8.4% for perflutren lipid microbubbles,[35] and 5% for sulfur hexafluoride lipid-type A microbubbles[36]). None of the experienced adverse events led to discontinuation of the study, and there were no abnormalities or significant changes or trends in vital signs, ECG, and measured laboratory tests. In addition, rates of adverse events were not increased at the higher tested doses. Because the rate of adverse events after $MB_{KDR}$ administration is also comparable to the reported rate for the nontargeted core microbubble BR38,[37] integrating binding ligands to the microbubble shell seems to be safe.

We also assessed the feasibility of USMI of KDR expression in ovarian and breast lesions using routine and clinically available ultrasound equipment and leveraging the unique resonating properties of microbubbles in an acoustic field at clinically used frequencies.[38-40] Except for 14% of patients with breast lesions in whom technical difficulties were encountered during the early technical optimization phase of the study, USMI was feasible in all subsequent patients. Quantification of breast lesion data suggested that the KDR-targeted USMI signal was up to approximately eight-fold higher in breast cancer compared with surrounding normal breast tissue.

Our study also showed that KDR-targeted USMI signal matched well with histologic KDR expression in both ovarian and breast lesions, suggesting for the first time that USMI allows noninvasive assessment of KDR expression in patients. Because the KDR-positive signal was graded semiquantitatively using different Likert scales for USMI and histology, we acknowledge that our matching analysis only represents a trend; however, it is a promising trend. We also acknowledge that anatomically correlating histology sections with the ultrasound imaging planes was difficult in some cases, in particular in ovarian lesions with a cystic component where it was difficult to determine the exact imaging plane on histology. Ongoing developments in three-dimensional USMI[41-43] may overcome some of these challenges in future clinical trials.

Because the background signal from freely circulating nonbound targeted microbubbles decreases quickly by a rapid systemic clearance through the reticuloendothelial system,[44,45] the KDR-targeted USMI signal could be observed as early as 7 minutes after $MB_{KDR}$ administration in many patients, with 13 minutes being

  

the optimal time point for 96% of ovarian and breast cancer lesions. This is a major advantage of USMI, making it an almost real-time bedside exam, compared with other emerging or existing molecular imaging techniques.[46] In addition, targeted imaging signal could be visualized for an average of 17 minutes in patients with ovarian or breast cancer (and possibly longer because we only tested up to 29 minutes after intravenous administration). This has additional practical significance because both ovaries and breasts (in particular, with the introduction of whole-breast imaging systems)[47,48] could be imaged with USMI after a single contrast agent injection in the future. Furthermore, ongoing technical developments will allow quasi–real-time assessment of targeted USMI signal without the need for waiting for nonbound contrast agent clearance,[49,50] further improving the clinical workflow and efficiency of USMI.

We acknowledge that our exploratory study with inclusion of only a limited number of patients was not powered to assess whether KDR-targeted USMI allows accurate differentiation between malignant and benign lesions. In addition, although malignant breast lesions were classified uniformly as ductal adenocarcinoma, there was a wide variety of different benign and malignant histologic entities in patients with ovarian lesions, reflecting the known preoperative difficulty in characterizing ovarian lesions as a result of the lack of specific imaging or other types of biomarkers. Our results show a trend that USMI may be useful in differentiating malignant from benign lesions, thereby possibly reducing unnecessary biopsies or surgeries in the future. Future multicenter trials are needed to test this hypothesis.

In conclusion, our study shows the successful clinical translation of USMI with $MB_{KDR}$, which is currently the only available clinical-grade molecularly targeted contrast agent. $MB_{KDR}$ has recently received Investigational New Drug approval from the US Food and Drug Administration to allow further clinical testing (ClinicalTrials.gov identifier: NCT02142608).[51] Targeted USMI is feasible and safe and allows for noninvasive detection of KDR expression in patients with ovarian and breast lesions. This strategy can be generalized to the detection and characterization of other cancers and to the use of other types of ultrasound contrast microbubbles targeted at other imaging biomarkers beyond KDR.

## AUTHORS' DISCLOSURES OF POTENTIAL CONFLICTS OF INTEREST

Disclosures provided by the authors are available with this article at jco.org.

## AUTHOR CONTRIBUTIONS

**Conception and design:** Jürgen K. Willmann, Amelie M. Lutz, Sanjiv S. Gambhir
**Financial support:** Jürgen K. Willmann, Sanjiv S. Gambhir
**Administrative support:** Jürgen K. Willmann, Sanjiv S. Gambhir
**Collection and assembly of data:** Jürgen K. Willmann, Lorenzo Bonomo, Antonia Carla Testa, Pierluigi Rinaldi, Sanjiv S. Gambhir
**Data analysis and interpretation:** Jürgen K. Willmann, Guido Rindi, Keerthi S. Valluru, Gianluigi Petrone, Maurizio Martini, Sanjiv S. Gambhir
**Manuscript writing:** All authors
**Final approval of manuscript:** All authors
**Accountable for all aspects of the work:** All authors

## REFERENCES


1. Berg WA, Bandos AI, Mendelson EB, et al: Ultrasound as the primary screening test for breast cancer: Analysis from ACRIN 6666. J Natl Cancer Inst 108:djv367, 2015
2. van Nagell JR Jr, DePriest PD, Ueland FR, et al: Ovarian cancer screening with annual transvaginal sonography: Findings of 25,000 women screened. Cancer 109:1887-1896, 2007
3. Deshpande N, Pysz MA, Willmann JK: Molecular ultrasound assessment of tumor angiogenesis. Angiogenesis 13:175-188, 2010
4. Kaneko OF, Willmann JK: Ultrasound for molecular imaging and therapy in cancer. Quant Imaging Med Surg 2:87-97, 2012
5. Korpanty G, Carbon JG, Grayburn PA, et al: Monitoring response to anticancer therapy by targeting microbubbles to tumor vasculature. Clin Cancer Res 13:323-330, 2007
6. Kiessling F, Fokong S, Koczera P, et al: Ultrasound microbubbles for molecular diagnosis, therapy, and theranostics. J Nucl Med 53:345-348, 2012
7. Laeseke PF, Chen R, Jeffrey RB, et al: Combining in vitro diagnostics with in vivo imaging for earlier detection of pancreatic ductal adenocarcinoma: Challenges and solutions. Radiology 277: 644-661, 2015
8. Lutz AM, Willmann JK, Drescher CW, et al: Early diagnosis of ovarian carcinoma: Is a solution in sight? Radiology 259:329-345, 2011
9. Lutz AM, Bachawal SV, Drescher CW, et al: Ultrasound molecular imaging in a human CD276 expression-modulated murine ovarian cancer model. Clin Cancer Res 20:1313-1322, 2014
10. Wang L, Li L, Guo Y, et al: Construction and in vitro/in vivo targeting of PSMA-targeted nanoscale microbubbles in prostate cancer. Prostate 73: 1147-1158, 2013
11. Foygel K, Wang H, Machtaler S, et al: Detection of pancreatic ductal adenocarcinoma in mice by ultrasound imaging of thymocyte differentiation antigen 1. Gastroenterology 145:885-894.e3, 2013
12. Leguerney I, Scoazec J-Y, Gadot N, et al: Molecular ultrasound imaging using contrast agents targeting endoglin, vascular endothelial growth factor receptor 2 and integrin. Ultrasound Med Biol 41: 197-207, 2015
13. Wei S, Fu N, Sun Y, et al: Targeted contrast-enhanced ultrasound imaging of angiogenesis in an orthotopic mouse tumor model of renal carcinoma. Ultrasound Med Biol 40:1250-1259, 2014
14. Hicklin DJ, Ellis LM: Role of the vascular endothelial growth factor pathway in tumor growth and angiogenesis. J Clin Oncol 23:1011-1027, 2005
15. Lyshchik A, Fleischer AC, Huamani J, et al: Molecular imaging of vascular endothelial growth factor receptor 2 expression using targeted contrast-enhanced high-frequency ultrasonography. J Ultrasound Med 26:1575-1586, 2007
16. Palmowski M, Huppert J, Ladewig G, et al: Molecular profiling of angiogenesis with targeted ultrasound imaging: Early assessment of antiangiogenic therapy effects. Mol Cancer Ther 7: 101-109, 2008
17. Rychak JJ, Graba J, Cheung AMY, et al: Microultrasound molecular imaging of vascular endothelial growth factor receptor 2 in a mouse model of tumor angiogenesis. Mol Imaging 6:289-296, 2007
18. Willmann JK, Lutz AM, Paulmurugan R, et al: Dual-targeted contrast agent for US assessment of tumor angiogenesis in vivo. Radiology 248:936-944, 2008
19. Willmann JK, Paulmurugan R, Chen K, et al: US imaging of tumor angiogenesis with microbubbles targeted to vascular endothelial growth factor receptor type 2 in mice. Radiology 246: 508-518, 2008
20. Lee DJ, Lyshchik A, Huamani J, et al: Relationship between retention of a vascular endothelial growth factor receptor 2 (VEGFR2)-targeted ultrasonographic contrast agent and the level of VEGFR2 expression in an in vivo breast cancer model. J Ultrasound Med 27:855-866, 2008
21. Anderson CR, Rychak JJ, Backer M, et al: scVEGF microbubble ultrasound contrast agents: A novel probe for ultrasound molecular imaging of tumor angiogenesis. Invest Radiol 45:579-585, 2010
22. Marshall D, Pedley RB, Boden JA, et al: Polyethylene glycol modification of a galactosylated streptavidin clearing agent: Effects on immunogenicity and clearance of a biotinylated anti-tumour antibody. Br J Cancer 73:565-572, 1996
23. Meyer DL, Schultz J, Lin Y, et al: Reduced antibody response to streptavidin through site-directed mutagenesis. Protein Sci 10:491-503, 2001

**24.** Pochon S, Tardy I, Bussat P, et al: BR55: A lipopeptide-based VEGFR2-targeted ultrasound contrast agent for molecular imaging of angiogenesis. Invest Radiol 45:89-95, 2010

**25.** Pysz MA, Foygel K, Rosenberg J, et al: Antiangiogenic cancer therapy: Monitoring with molecular US and a clinically translatable contrast agent (BR55). Radiology 256:519-527, 2010

**26.** Bachawal SV, Jensen KC, Lutz AM, et al: Earlier detection of breast cancer with ultrasound molecular imaging in a transgenic mouse model. Cancer Res 73:1689-1698, 2013

**27.** Bzyl J, Lederle W, Rix A, et al: Molecular and functional ultrasound imaging in differently aggressive breast cancer xenografts using two novel ultrasound contrast agents (BR55 and BR38). Eur Radiol 21:1988-1995, 2011

**28.** Sugimoto K, Moriyasu F, Negishi Y, et al: Quantification in molecular ultrasound imaging: A comparative study in mice between healthy liver and a human hepatocellular carcinoma xenograft. J Ultrasound Med 31:1909-1916, 2012

**29.** Pysz MA, Machtaler SB, Seeley ES, et al: Vascular endothelial growth factor receptor type 2-targeted contrast-enhanced US of pancreatic cancer neovasculature in a genetically engineered mouse model: Potential for earlier detection. Radiology 274: 790-799, 2015

**30.** Baetke SC, Rix A, Tranquart F, et al: Squamous cell carcinoma xenografts: Use of VEGFR2-targeted microbubbles for combined functional and molecular US to monitor antiangiogenic therapy effects. Radiology 278:430-440, 2016

**31.** Grouls C, Hatting M, Rix A, et al: Liver dysplasia: US molecular imaging with targeted contrast agent enables early assessment. Radiology 267: 487-495, 2013

**32.** Fischer AH, Jacobson KA, Rose J, et al: Hematoxylin and eosin staining of tissue and cell section. CSH Protoc 2008:pdb.prot4986, 2008

**33.** European Medicines Agency: ICH topic E 8: General considerations for clinical trials. http://www.ema.europa.eu/docs/en_GB/document_library/Scientific_guideline/2009/09/WC500002877.pdf

**34.** GE Healthcare: Optison. https://promo.gelifesciences.com/gl/OPTISONIMAGING/misc/Updated-Optison-PI-10-21-14.pdf

**35.** Lantheus Medical Imaging: Definity. http://www.definityimaging.com/why-safety.html

**36.** Bracco Imaging: Lumason. http://imaging.bracco.com/sites/braccoimaging.com/files/technica_sheet_pdf/Lumason%20SDS.pdf

**37.** Schneider M, Anantharam B, Arditi M, et al: BR38, a new ultrasound blood pool agent. Invest Radiol 46:486-494, 2011

**38.** de Jong N, Bouakaz A, Frinking P: Basic acoustic properties of microbubbles. Echocardiography 19:229-240, 2002

**39.** Unnikrishnan S, Klibanov AL: Microbubbles as ultrasound contrast agents for molecular imaging: preparation and application. AJR Am J Roentgenol 199:292-299, 2012

**40.** Willmann JK, Kimura RH, Deshpande N, et al: Targeted contrast-enhanced ultrasound imaging of tumor angiogenesis with contrast microbubbles conjugated to integrin-binding knottin peptides. J Nucl Med 51:433-440, 2010

**41.** Wang H, Kaneko OF, Tian L, et al: Three-dimensional ultrasound molecular imaging of angiogenesis in colon cancer using a clinical matrix array ultrasound transducer. Invest Radiol 50:322-329, 2015

**42.** Wang H, Lutz AM, Hristov D, et al: Intra-animal comparison between three-dimensional molecularly targeted us and three-dimensional dynamic contrast-enhanced US for early antiangiogenic treatment assessment in colon cancer. Radiology 282:443-452, 2017

**43.** Zhou J, Wang H, Zhang H, et al: VEGFR2-targeted three-dimensional ultrasound imaging can predict responses to antiangiogenic therapy in preclinical models of colon cancer. Cancer Res 76: 4081-4089, 2016

**44.** Willmann JK, Cheng Z, Davis C, et al: Targeted microbubbles for imaging tumor angiogenesis: Assessment of whole-body biodistribution with dynamic micro-PET in mice. Radiology 249:212-219, 2008

**45.** Streeter JE, Dayton PA: An in vivo evaluation of the effect of repeated administration and clearance of targeted contrast agents on molecular imaging signal enhancement. Theranostics 3:93-98, 2013

**46.** Boellaard R, Delgado-Bolton R, Oyen WJG, et al: FDG PET/CT: EANM procedure guidelines for tumour imaging: Version 2.0. Eur J Nucl Med Mol Imaging 42:328-354, 2015

**47.** Kaplan SS: Automated whole breast ultrasound. Radiol Clin North Am 52:539-546, 2014

**48.** Kelly KM, Dean J, Comulada WS, et al: Breast cancer detection using automated whole breast ultrasound and mammography in radiographically dense breasts. Eur Radiol 20:734-742, 2010

**49.** Wang S, Hossack JA, Klibanov AL, et al: Binding dynamics of targeted microbubbles in response to modulated acoustic radiation force. Phys Med Biol 59:465-484, 2014

**50.** Pysz MA, Guracar I, Tian L, et al: Fast microbubble dwell-time based ultrasonic molecular imaging approach for quantification and monitoring of angiogenesis in cancer. Quant Imaging Med Surg 2: 68-80, 2012

**51.** Abou-Elkacem L, Bachawal S V, Willmann JK: Ultrasound molecular imaging: Moving toward clinical translation. Eur J Radiol 84:1685-1693, 2015

## *Affiliations*

**Jürgen K. Willmann**, **Keerthi S. Valluru**, **Amelie M. Lutz**, and **Sanjiv S. Gambhir**, Stanford University, Stanford, CA; and **Lorenzo Bonomo**, **Antonia Carla Testa**, **Pierluigi Rinaldi**, **Guido Rindi**, **Gianluigi Petrone**, and **Maurizio Martini**, Universitary Policlinic A. Gemelli-Foundation, Catholic University, Rome, Italy.

## *Support*

Supported by the National Institutes of Health (NIH) and Bracco (Geneva, Switzerland). J.K.W. and A.M.L. were supported in part by NIH Grant No. R01 CA155289 (J.K.W.). This work was also supported in part by the Canary Foundation (J.K.W., S.S.G.), NCI CCNE-T U54 CA151459 (S.S.G.), and NCI CCNE-TR U54 CA119367 (S.S.G).

  

## AUTHORS' DISCLOSURES OF POTENTIAL CONFLICTS OF INTEREST

**Ultrasound Molecular Imaging With BR55 in Patients With Breast and Ovarian Lesions: First-in-Human Results**

*The following represents disclosure information provided by authors of this manuscript. All relationships are considered compensated. Relationships are self-held unless noted. I = Immediate Family Member, Inst = My Institution. Relationships may not relate to the subject matter of this manuscript. For more information about ASCO's conflict of interest policy, please refer to www.asco.org/rwc or ascopubs.org/jco/site/ifc.*

**Jürgen K. Willmann**
**Consulting or Advisory Role:** Bracco Diagnostics, SonoVol
**Speakers' Bureau:** Siemens Healthcare Diagnostics, Bracco Diagnostics
**Research Funding:** Bracco Diagnostics (Inst), Siemens Healthcare Diagnostics (Inst), Philips Healthcare (Inst), GE (Inst)

**Lorenzo Bonomo**
No relationship to disclose

**Antonia Carla Testa**
No relationship to disclose

**Pierluigi Rinaldi**
No relationship to disclose

**Guido Rindi**
**Speakers' Bureau:** Novartis Pharma, Ipsen Pharma

**Keerthi S. Valluru**
No relationship to disclose

**Gianluigi Petrone**
No relationship to disclose

**Maurizio Martini**
No relationship to disclose

**Amelie M. Lutz**
**Consulting or Advisory Role:** Bracco Diagnostics (I)

**Sanjiv S. Gambhir**
**Stock or Other Ownership:** Endra, Cellsight Technologies, Vor, ImaginAB, MagArray, PureTech, Grail, Verily, Cytomx, Rio, Reflexion Medical, Click Diagnostics
**Honoraria:** Visualsonics, Infinitus, Puretech, Click Diagnostics, Bracco Diagnostics, Vor
**Consulting or Advisory Role:** Bracco Diagnostics, Verily, Grail, Visualsonics, ImaginAB, Puretech, Vor, Infintius, Cellsight Technologies, Endra
**Research Funding:** General Electric Healthcare (Inst), Philips Healthcare, Siemens Healthcare Diagnostics (Inst), Bracco Diagnostics (Inst), Verily
**Patents, Royalties, Other Intellectual Property:** Molecular imaging patents

***Acknowledgment***

We acknowledge Arnaldo Carbone, MD, and Gianfranco Zannoni, MD, for pathology work; Domenica Perni for skillful histology technical assistance; Ilaria De Blasis, MD, Bruna Virgilio, MD, and Francesca Moro, MD for their assistance in examining the patients with ovarian tumors and collecting data; and Tina Pasciuto, MS, for the assistance in collecting data (all at Università Cattolica del Sacro Cuore). We also thank Jarrett Rosenberg, PhD, for his assistance with the statistical analysis and Jim Strommer for his help in designing Figure 1 (both at Stanford University).